Electroblotting through enzymatic membranes to enhance molecular tissue imaging

William T. Andrews[1], Adrianna Bickner[1], Fernando Tobias[3], Kendall A. Ryan[1], Merlin L. Bruening[1, 2], Amanda B. Hummon[3]*

[1]Department of Chemistry and Biochemistry

[2]Department of Chemical and Biomolecular Engineering

University of Notre Dame

Notre Dame, IN 46556

[3]Department of Chemistry and Biochemistry

Comprehensive Cancer Center

The Ohio State University

Columbus, OH 43210

*Corresponding author

Email: hummon.1@osu.edu

Phone: 614-688-2580

Running Title: Electroblotting for protein imaging

Keywords: peptide extraction, MALDI, imaging, tissue imaging, on-tissue digestion, tryptic digestion, molecular scanner, electroblot, electrotransfer, membranes, pepsin

Abstract:

MALDI-TOF mass spectrometry imaging (MSI) is a powerful tool for studying biomolecule localization in tissue. Protein distributions in tissue provide important histological information; however, large proteins exhibit a high limit of detection in MALDI-MS when compared to their corresponding smaller proteolytic peptides. As a result, several techniques have emerged to digest proteins into more detectable peptides for imaging. Digestion is typically accomplished through trypsin deposition on the tissue, but this technique increases the complexity of the tissue microenvironment, which can limit the number of detectable species. This proof-of-principle study explores tryptic tissue digestion during electroblotting through a trypsin-containing membrane. This approach actively extracts and enzymatically digests proteins from mouse brain tissue sections, while simultaneously reducing the complexity of the tissue microenvironment (compared to trypsin deposition on the surface) to obtain an increased number of detectable peptide fragments. The method does not greatly compromise spatial location or require expensive devices to uniformly deposit trypsin on tissue. Using electrodigestion through membranes, we detected and tentatively identified several tryptic peptides that were not observed after on-tissue digestion. Moreover, the use of pepsin rather than trypsin in digestion membranes allows extraction and digestion at low pH to detect peptides from a complementary subset of tissue proteins. Future studies will aim to further improve the method, including changing the substrate membrane to increase spatial resolution and the number of detected peptides.

Introduction:

Matrix-Assisted Laser Desorption/Ionization (MALDI) mass spectrometry imaging (MSI) is a promising tool for diagnosing diseases in humans,[1, 2] examining the distribution of neuropeptides in brain tissues,[3, 4] and mapping the penetration of drugs and metabolites in tissues and three-dimensional cultures.[5-7] In a single experiment, this technique allows the user to detect a wide range of analytes and study their localization within a tissue or cell culture.[8, 9] However, when imaging the distribution of larger proteins using this technique, detection limits are high because of both the nature of the mass detector in the instrument [10, 11] and ion suppression due to the complexity of the tissue microenvironment.[12, 13]

On-tissue tryptic digestion often enhances MSI detection and identification of larger proteins.[8, 14] In this method, trypsin applied to the tissue surface catalyzes the cleavage of proteins into peptides for easier detection. Nevertheless, the presence of lipids and metabolites as well as autolysis products from deposited trypsin complicate the mass spectrum from such tissue surfaces. These molecules also suppress ionization, and hence signals, for analytes of interest.[15] In addition, on-tissue digestion requires cumbersome and time-consuming sample preparation steps, as well as expensive deposition devices.[10]

An alternative, complementary approach is electroblotting through a trypsin membrane prior to analysis of the blot using MALDI MSI (**Figure 1**). This method affords tryptic digestion while simultaneously reducing the complexity of the tissue microenvironment through actively extracting analytes of interest.[16] Several manuscripts described this strategy as part of a “molecular scanner” approach for imaging 2-D gels,[17, 18] but it has yet to be thoroughly assessed when blotting whole tissue sections.[11] Moreover, the membranes employed in this study contain two orders of magnitude more

immobilized protease than membranes used in most prior studies.[19-22]

Our previous research showed that actively extracting analytes of interest to reduce the complexity of the tissue microenvironment is an effective method for analyzing peptides using MALDI-TOF MSI.[23, 24] However, electroblotting through a trypsin membrane could accomplish this feat while simultaneously digesting proteins into more detectable peptides without the use of an expensive trypsin deposition device. Furthermore, one could envision the addition of other specialized membranes to the blotting apparatus to provide added functionality such as lipid removal, selective protein capture, or peptide tagging simultaneously with digestion during blotting. This study investigates the effectiveness of electroblotting through tryptic and peptic membranes, termed electrodigestion, to detect peptides while retaining biomolecule spatial localization. Compared to traditional tissue blotting[25] and on-tissue tryptic digestion methods, electrodigestion does not increase the complexity of the sample as it actively extracts analytes of interest and minimizes contaminating trypsin autolysis products. This method allows a similar number of identified tryptic peptides when compared to on-tissue tryptic digestion.[26] Moreover, electrodigestion through peptic membranes at low pH yields a different subset of charged species that migrate through the membrane and undergo digestion.

Experimental:

Materials and reagents. Proteomics grade trypsin was obtained from Promega (Madison, WI), and pepsin from porcine gastric mucosa (lyophilized powder, 3200–4500 units per mg protein) was purchased from Sigma Aldrich. Bovine serum albumin (BSA) conjugated to Alexa Fluor™ 488 (BSA-488) was purchased from Invitrogen (Carlsbad, CA).

Membranes containing electrostatically bound trypsin or pepsin were prepared as described previously [21, 27] with the following reagents: trypsin from porcine pancreas type IX-S (lypholized powder), poly(sodium 4-styrenesulfonate) (M_w~ 70 000) (PSS), NaCl and HCl purchased from Sigma Aldrich (St Louis, Missouri). A 2.5 × 3.5 cm piece of nylon membrane (LoProdyne LP, pore size 1.2 μm, 110 μm thickness, Pall corporation, Port Washington, New York) was cleaned with UV-ozone for 10 min and inserted into a home-made aluminum holder attached to a peristaltic pump. 100 mL of water was passed through the membrane, and then 100 mL of 20 mM poly(sodium 4-styrenesulfonate) in 0.5 M NaCl adjusted to pH 2.3 was circulated through the system for 20 min at 2 mL min^{-1}. 100 mL of water was then passed through the membrane before circulating 100 mL of a 1 mg mL^{-1} trypsin solution through the membrane at 2 mL min^{-1} for 1 hour. Lastly, 100 mL of 1 mM HCl was passed through the membrane, which was then dried under nitrogen and stored until use.

Polyvinylidene fluoride (PVDF) membranes for protein blotting were purchased from Bio-Rad Laboratories (Des Plaines, IL). In some cases, we used a LoProdyne nylon membrane modified with a poly(acrylic acid) (PAA)/ polyethyleneimine (PEI) multilayer film as a blotting substrate. Compared to PVDF, these modified membranes improved peptide elution after electroblotting. PAA/PEI/PAA/PEI coating was performed as described previously.[28] All unspecified reagents were purchased from Sigma Aldrich (St. Louis, MO). Mouse tissue was acquired by generous donation from the M. Sharon Stack laboratory at the University of Notre Dame. The tissues were unused brains from mice sacrificed under IACUC approval. All mouse brain tissues were sectioned into consecutive 15 μm slices using a cryostat sectioning device at -20˚C and mounted on aluminum foil. Tissue sections were then stored at -20˚C. Prior to blotting, all mouse brain tissue sections were washed in 70%, 90% and 95% ethanol for one minute to remove lipid

species and then dried in a desiccator. All tissue blots were conducted with a minimum of three technical replicates from the same mouse; however, different mice were used for each experiment.

Examining spatial resolution through blotting from a polyacrylamide gel. Sodium dodecyl sulfate polyacrylamide gel electrophoresis was performed with fluorescently labelled BSA-488, and the resulting protein band was identified and imaged using a phone camera, a handheld UV lamp (model UVGL-58 from UVP, San Gabriel, CA) and a light box. Protein transfer from the gel was performed by electroblotting through a trypsin membrane onto a PVDF capture membrane. The transfer buffer was 19.2 mM glycine and 2.5mM Tris in 20% methanol, and electrodigestion was performed at 6 V for 3 h. Immediately after quickly imaging the blot, the membrane was coated with DHB matrix using the above method. In preparation for MALDI-TOF MSI, the membrane was affixed to a stainless-steel target using conductive double-sided tape and dried under vacuum. Imaging was performed with a Bruker UltrafleXtreme MALDI mass spectrometer (Billerica, MA) using a laser attenuation of 65%, a Smartbeam parameter set of 2_small, and calibration using Bruker peptide standard II. Gel and membrane fluorescence images were processed using Image J software (NIH) [29] and compared with the mass spectrometry image. Each image was converted to grayscale, contrast enhanced at 0.5% uniformly across the images, inverted, and cropped to focus on the BSA-488 band.

Mass spectrometry. Initial tissue imaging experiments were conducted using a Bruker UltrafleXtreme MALDI mass spectrometer with a laser spot size of 150 μm at a 1000 Hz sampling frequency. A spot size of 150 μm was chosen due to the large size of the tissue sample and the need to use a lower laser power (~35% with attenuation) so as to not desorb the PVDF membrane. Ion cyclotron resonance (ICR) MSI experiments

were conducted on a Bruker Solarix 15T FT-ICR equipped with a MALDI source. Prior to MALDI MSI analysis all samples were coated with 10 µg/µL of 2,5-dihydroxybenzoic acid (DHB) matrix solution (50% H_2O, 50% acetonitrile, with 0.1% TFA) using an HTX Imaging TM-Sprayer (Chapel Hill, NC). All MALDI experiments were calibrated using a Bruker Peptide Calibration standard. DHB was chosen over other matrices, as it displayed reduced background signal from matrix clusters. Samples were coated with 8 passes at 80˚C at a 0.1 mL/min flow rate, track spacing of 2 mm, pressure of 10 psi, gas flow of 3 L/min, and 1000 mm/min velocity. MALDI-TOF MSI of PVDF collection membranes required low laser power to avoid desorbing and/or ionizing the membrane. Higher laser power was used for MALDI FT-ICR imaging experiments, as desorbed PVDF was filtered out by the quadrupole mass filter. Detectable peaks were defined as having a signal-to-noise ratio greater than three sigma. Imaging data was acquired using flexImaging software, and queried imaging data was analyzed using flexAnalysis and SCiLS Lab v2016b (Bruker). MS/MS experiments on the TOF/TOF instrument were conducted using post-source decay, as additional collision energy eliminated all signal for peptide fragments.

After electrodigestion with PAA/PEI/PAA/PEI-coated nylon capture membranes, and peptide extraction, nano-ultrahigh performance liquid chromatography MS/MS was performed to identify peptides. For peptide extraction, the capture membrane was soaked in 100 µL of 0.03% zwittergent 3-16 (Millipore Sigma) in 10 mM ammonium bicarbonate for 30 seconds while vortexing. The eluate was then treated with Thermo HiPPR Detergent Removal Spin Columns followed by desalting with Pierce C18 Spin Columns. LC-MS/MS was performed on a Q-Exactive Hybrid Quadrupole–Orbitrap instrument (Thermo, San Jose, CA), and data analysis was performed using MaxQuant. LC-MS/MS and MaxQuant analysis occurred as previously described[30] using *Mus Musculus* (Mouse) proteome (55,197 proteins) in the database search.

Semi-dry tissue blotting. Tissue blots were conducted for three hours onto a PVDF collection surface using a modified transfer process originally established by Fournaise and Chaurand.[25] Prior to MALDI MSI, PVDF collection membranes were mounted onto Indium-Tin-Oxide (ITO)-coated glass slides using double-sided conductive tape obtained from 3M (Plymouth, IN).

Electroblotting and Electrodigestion. Using a modified protocol originally established by Rohner, Staab, and Stoeckli,[11] electroblots occurred in an XCell SureLock Mini-Cell with Novex Blot Module by Invitrogen (Carlsbad, CA). A pH 8 transfer buffer containing 2.5 mM Tris, 19.2 mM glycine, 50 mM ammonium bicarbonate and 0.01% SDS was used to carry out electrotransfer as well as tryptic digestion. During the electroblotting, the temperature increased from room temperature to 35 degrees Celsius, which helps to facilitate the enzymatic digestion. For pepsin digestion, a solution of 1.5% formic acid in water was substituted as a transfer buffer. Non-enzymatic electrotransfers utilized bare nylon membranes that were sandwiched between the tissue sample and the PVDF collection surface in the stack. All electroblots and electrotransfers were conducted under 6V for three hours.

On-tissue digestion. Proteomics grade trypsin (Promega) was applied to tissue sections using an HTX Imaging TM-Sprayer (Chapel Hill, NC). On-tissue tryptic digestion was performed according to the HTX Imaging manufacturer's specifications before MALDI MSI analysis.

Data Deposition. Mass spectrometry data files have been uploaded to public servers. The high resolution FT-ICR data has been uploaded to the Metaspace platform (https://metaspace2020.eu). The TOF data has been uploaded to ProteomeXchange (http://www.proteomexchange.org).

Results and Discussion:

This study investigates electroblotting through trypsin-containing membranes to digest proteins while minimizing analyte ion suppression in subsequent MALDI-MSI due to actively extracting the analytes of interest. We first compare electroblotting to the traditional tissue blotting methods utilized by Fournaise and Chaurand[25] and then assess whether the inclusion of a trypsin membrane in the electroblotting apparatus leads to effective digestion of proteins migrating from the tissue. Subsequent experiments compare electrodigestion to on-tissue tryptic proteolysis in terms of spectral quality and the presence of contaminants. Lastly, we demonstrate the flexibility of this method by implementing membranes containing immobilized pepsin rather than trypsin.

Comparison of Tissue Blotting and Electroblotting to Detect Endogenous Neuropeptides.

Mouse brain tissue sections were electroblotted through non-functionalized nylon membranes and compared to tissue blots obtained using a traditional semi-dry blotting method (**Figure 2**). Complementary hematoxylin and eosin stains were not acquired as the samples needed to be mounted on conductive aluminum foil. In the semi-dry blotting method, the nylon transfer membrane between the dry tissue and the PVDF collection surface was imbibed with 150 mM ammonium formate buffer to facilitate diffusion in the absence of an electric field. With both the semi-dry tissue blot approach illustrated in **Figure 2a** and the electroblot method shown in **Figure 2b**, endogenous peptides collect on PVDF membranes. After blotting, we coated the PVDF substrates with DHB matrix and analyzed the blotted species using MALDI-TOF MSI. It is important to note that MALDI-TOF MSI of PVDF collection membranes requires low laser power to avoid ablating the membrane. As a result, spectra obtained from PVDF collection surfaces have limited signal intensity. **Figure 3** provides examples of MALDI-MSI spectra and

images of both semi-dry blotted and electroblotted endogenous brain tissues. Endogenous peptides collected onto the blotting substrate were tentatively identified by comparing their *m/z* value with corresponding values for common endogenous peptides (**Table 1**).[30] Some of the putatively identified peptides include those with 596.3, 605.8, 662.8, 734.8, 761.9, and 806.9 *m/z*. PVDF collection surfaces from electroblotting show more intense signals for most of these species (~2-fold higher for 734.8 and 761.9 *m/z*) compared to collection surfaces from traditional semi-dry blotting. Although several neuropeptides were detected following both blotting methods, signals at 605.8 and 806.9 *m/z* were only detectible following electroblotting. The reduced number of analytes obtained with semi-dry blotting is possibly due to low analyte affinity for the blotting substrate, as previously proposed by Fournaise and Chaurand.[25] Electroblotting may push the analytes onto the substrate despite low affinity. When compared to passive blotting, the applied electric field in electroblotting results in more rapid movement of analytes to the PVDF collector. This should limit lateral diffusion, as illustrated by the limited diffusion of the diagnostic lipids phosphatidylcholine PC (34:1), *m/z* 760.609, and PC (32:0), *m/z* 734.591, detected via FT-ICR MSI (**Figure 4**). A no tissue control was also analyzed and no signal was observed after a three-hour blotting period. Estimation of the extent of lateral diffusion during electroblotting and MSI was conducted by measuring the neocortex in the H&E stain and MSI images, as displayed in **Figure S1.**

Figure 4 indicates that electroblotting preserves spatial resolution in lipid imaging, and prior studies show that proteins and lipids often show similar spatial patterns. [31] To examine whether electrodigestion and imaging of the resulting peptides preserve the spatial distribution of the parent protein, we imaged the band of a fluorescent protein after both electrophoresis and subsequent electrodigestion. Figure S2a shows the fluorescence image of a BSA-488 band in a polyacrylamide gel, and Figures S2b and S2c show fluorescence and MALDI-TOF images, respectively, of the

same band after electrodigesting it to a PVDF membrane. The fluorescence from the PVDF membrane has a higher signal-to-noise ratio than the fluorescence from the gel (presumably due to the lower background fluorescence from PVDF). Nevertheless, the shape of the band on PVDF is essentially the same as that of the band in the gel. Even with the increased fluorescence signal-to-noise ratio on PVDF, the width of the band in Figure S2b is 5.1 mm, only 0.1 mm wider than the band in the gel (Figure S2a). MALDI-TOF MSI is less sensitive than fluorescence, so the band in Figure S2c appears narrower (width of 4.3 mm) than in the fluorescence images. The shape is similar to that in the fluorescence images and corresponds to the most intense areas of the protein band. The similar spot sizes and shapes in all the images in Figure S2 suggest that electrodigestion retains spatial resolution at around the 100-μm scale.

Utilization of Trypsin Membranes to Create Tryptic Peptides from Electroblotting Endogenous Proteins

To digest electroblotted endogenous proteins into peptides and then map these peptides, we employed the same experimental design depicted in **Figure 2b**, but with nylon membranes containing immobilized trypsin. **Figure 5** displays MALDI-MS spectra of PVDF collection surfaces after electroblotting mouse brain tissue through trypsin-modified or bare nylon membranes. The normalization for these images was performed using the total ion count for both the electroblotted and semi-dry blotted samples. When compared to electroblotting through nylon membranes, electroblotting through trypsin membranes yields unique peptides. In addition, the ion maps suggest some of these peptides are concentrated in distinct spatial regions (**Figure 5**). These results indicate that electrodigestion does not compromise the spatial localization of these peptides with respect to their native protein counterparts. Distinct spatial localization observed in

unblotted mouse brain tissue sections (**Figure S3**) also appears to be conserved after electrodigestion, although some lateral diffusion occurs during the electroblotting.

Importantly, due to the absence of autolysis products, electrodigestion produces comparable spectra when compared to on-tissue digestion methods, and minimal signal from autolysis products. **Figure 6** compares on-tissue tryptic digestion and electrodigestion images of mouse brain tissue sections. Electrodigestion yields several peptides, 707, 759, 809, and 1198 *m/z*, that were not detected following on-tissue tryptic digestion. **Table S2** gives tentative identifications of these peptides based on mass spectra of proteins digested under non-reducing conditions.[32] Several species that were detected following both on-tissue and electrodigestion have conserved spatial localization. Species that were abundant on the perimeter of the tissue after on-tissue digestion were also observed along the tissue perimeter after electrodigestion, suggesting that electrodigestion tryptically digests proteins without compromising their relative localization within the tissue sample. Although several tryptic peptides were unique to electrodigestion, some peptide signals were detected only after on-tissue digestion. Species observed at 773.8 and 1100.0 *m/z* were present in the on-tissue digest samples but were not detected after electrodigestion. These species yielded no tentative identifications when comparing the observed *m/z* to the literature values. They may migrate poorly in electrodigestion or have a low affinity for our blotting substrate.

Trypsin autolysis products may complicate mass spectra and cause ion suppression, so we examined mass spectra for evidence of trypsin autolysis. Four peaks corresponding to tryptic autolysis products were observed in the on-tissue digest spectra at 634, 650, 749, and 760 *m/z* (see **Table S3** and **Figure S4**). These species are present in the surrounding areas of the digested tissue, suggesting that they are

indeed from the autolysis of trypsin. We analyzed the same *m/z* values in spectra obtained after electrodigestion; however, no peaks corresponding to 650 or 749 *m/z* appeared. Although electrodigestion spectra contained 634 and 760 *m/z* peaks, ion maps for these species show distinct spatial localization in the mouse brain and were not detected from the area surrounding the tissue. This localization suggests that these species may be native-protein tryptic peptides that are normally not observed due to the presence of autolysis products after on-tissue tryptic digestion. Tandem MS/MS analysis of these two species was conducted to definitively confirm these findings (**Figure S5**). Differences in fragmentation spectra for 634 *m/z* obtained with on-tissue and electrodigestion suggest that these are indeed two different species. Although there are similarities in fragmentation spectra for 760 *m/z*, differences in the masses for the fragment ions indicate that these species should also be different.

Electrodigestion Utilizing FT-ICR Mass Spectrometry Coupled With LC-MS/MS Analysis

MALDI-TOF MSI analysis of PVDF collection membranes revealed several limitations, most notably, laser power. When using the time-of-flight instrument, increased laser power caused desorption and ionization of the membrane, resulting in noisy spectra. For this reason, we repeated our trypsin electrodigestion experiment and analyzed the PVDF collection surfaces on a Bruker Solarix 15T FT-ICR. In comparison to a time-of-flight instrument, the FT-ICR has more sophisticated ion optics, such as a quadrupole and octopole, which seemed to remove desorbed PVDF species before reaching the mass detector, allowing the use of increased laser power and desorption of more peptides. **Figure 7** displays the overall average spectrum for one of the PVDF collection surfaces after electrodigestion through a trypsin membrane. Heat maps for several unique peptides are also displayed, showing distinct spatial localization. As

opposed to MALDI-TOF analysis where tens of unique peptides were observed, FT-ICR analysis yielded over 100 unique peptides, as more peptides could now be desorbed and ionized. Of these 100 unique peptides, 24 of them were sequenced by LC-MS/MS from an electrodigestion of a consecutive brain section on a PAA/PEI/PAA/PEI collection surface (**Table S4**). **Figure 7** gives heat maps for several of these peptides. Because of the increased laser intensity, we detect many more peptides using the FT-ICR rather than the MALDI-TOF instrument. In addition, the superior mass resolution of the ICR allows us to identify many of them by accurate mass by coupling with LC-MS/MS. These data demonstrate both the potential and versatility of the electrodigestion method.

Electroblotting and Digestion under Acidic Conditions Using Pepsin-Containing Membranes

The experimental procedure depicted in **Figure 1** was repeated utilizing pepsin-containing membranes (as opposed to trypsin membranes) to illustrate the flexibility of the method. This change of enzyme also allows us to conduct electrodigestion in completely different conditions because pepsin digests proteins at a pH of 2-3, whereas trypsin is most active at a pH of 7-8. Many more proteins will be positively charged at pH 3 than at pH 7, so peptic electrodigestion may yield more proteolytic peptides than tryptic electrodigestion. However, pepsin does not cleave proteins in a highly site-specific manner, so peptic peptide identification is difficult. For this reason, we did not yet attempt to identify peptides after pepsin electrodigestion.

Mouse brain tissue sections were electroblotted through bare nylon and immobilized-pepsin membranes onto PVDF collection surfaces that were then coated with DHB matrix and analyzed using MALDI-TOF IMS. **Figure 8** displays overall average spectra from the two collection surfaces, as well as heat maps generated from such spectra. A direct comparison of the two spectra shows an increased number of

species detected after pepsin electrodigestion when compared to electroblotting through a bare nylon membrane (**Figure S6**). **Figure 8** displays heat maps for four of these species, 553.2, 575.2, 731.2, and 1325.5 *m/z*, which were only detected after pepsin electrodigestion. In addition, these species display distinct spatial localizations, suggesting that they are peptides resulting from enzymatic digestion of endogenous proteins. Thus, this method is compatible with different enzymes and may be customized to accommodate a variety of enzymes. In the future, FT-ICR analyses will likely reveal many more peptic peptides and enable their identification.

Conclusions:

This study demonstrates that electrodigestion is a promising alternative to on-tissue tryptic digestion methods and has potential as a complementary imaging modality. Electroblotting provides improved analyte retention and spatial localization compared to traditional semi-dry tissue blotting. In addition, utilization of a trypsin membrane in the electroblotting scheme allows for proteolysis of native proteins in tissue without the added microenvironment complexity that results from deposition of trypsin onto the tissue. As a result, electrodigestion with subsequent MALDI MSI analysis yields spectra with fewer peaks corresponding to trypsin autolysis products when compared to spectra obtained after on-tissue tryptic digestion. Moreover, both trypsin and pepsin-loaded membranes are effective for this strategy, and pepsin-containing membranes may yield a complementary set of peptides due to electroblotting at low pH. These promising results could potentially allow the utilization of multiple proteases at the same time, without complicating the resulting spectra with autolysis products. Although limited laser ablation on MALDI-TOF systems with this method reduces signal intensity, other instrumentation such as an FT-ICR spectrometer can overcome this problem.

While electrodigestion provides a promising potential alternative approach to on-tissue enzymatic digestion, improvements to the method are needed. In particular, modification of the membrane to minimize PVDF ablation will allow for higher laser power, a smaller laser spot and improved spatial resolution. Previous work by the Chaurand group with alternative substrates like nitrocellulose slides[25] provides a starting point for these optimization studies. With additional optimization, we hope that this approach will be of utility to the field of imaging mass spectrometry.

Acknowledgements:

This research was supported by an NIA award (1R21AG062144) to ABH and MB. ABH was supported by the National Institutes of Health (R01GM110406). KAR was supported by the National Science Foundation (CHE1903967).The UltrafleXtreme instrument (MALDI-TOF-TOF) was acquired through National Science Foundation award #1625944. The 15 T Bruker SolariXR FT-ICR instrument was supported by NIH Award Number Grant S10 OD018507. We gratefully acknowledge the assistance of the Notre Dame Mass Spectrometry and Proteomics Facility (MSPF), Proteomics Shared Resource (PSR) in the Campus Chemical Instrument Center at the Ohio State University, and the generous donation of tissue samples by the M. Sharon Stack laboratory at the University of Notre Dame, as well as Weijing Liu, Hui Yin Tan and Xin Liu at the University of Notre Dame for providing enzymatic membranes, coating samples, and providing helpful discussions and support.

Figures

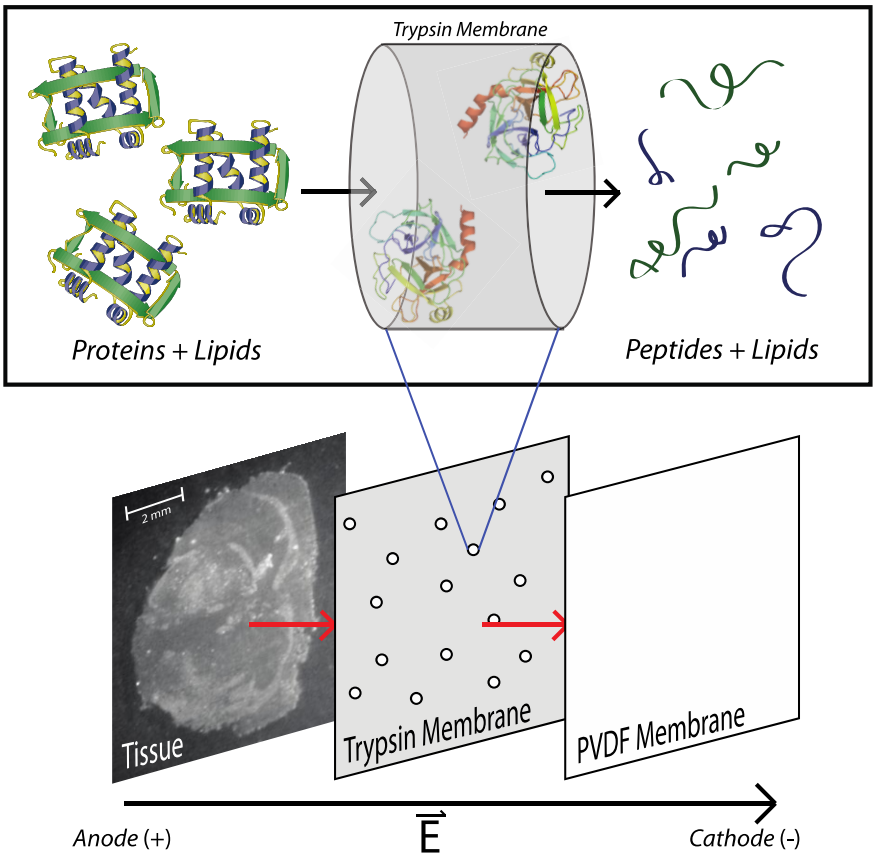

Figure 1. Basic concept of the electroblotting/digestion approach. An applied electric field leads to migration of positively charged species through a membrane modified with electrostatically bound trypsin. The resulting peptides are then collected on a PVDF membrane and imaged using MALDI-TOF MSI.

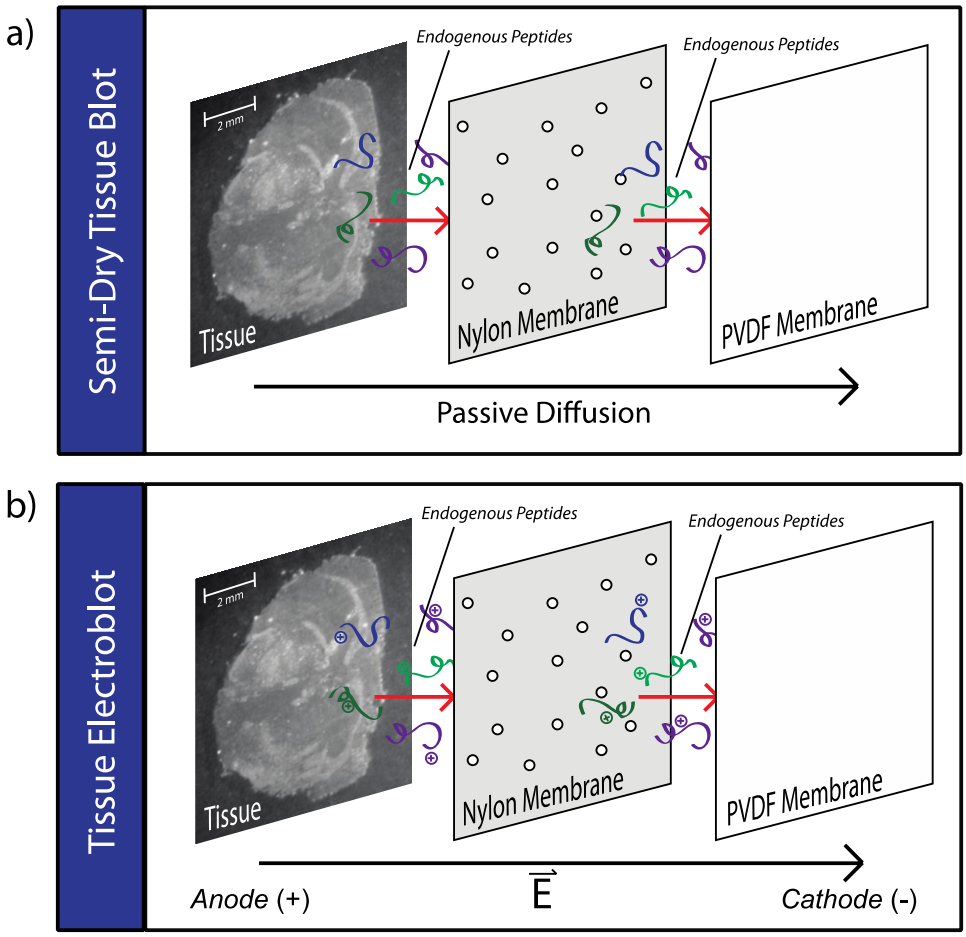

Figure 2. Schemes of semi-dry and electroblotting methods. Consecutive mouse brain tissue sections were blotted through porous nylon membranes onto PVDF collection substrates. (a) In a traditional semi-dry approach, endogenous peptides move to the PVDF substrate via passive diffusion. (b) In electroblotting, charged peptides at a pH of 8 were subjected to a 6 V electric potential, allowing migration through the nylon membrane onto the PVDF collection membrane.

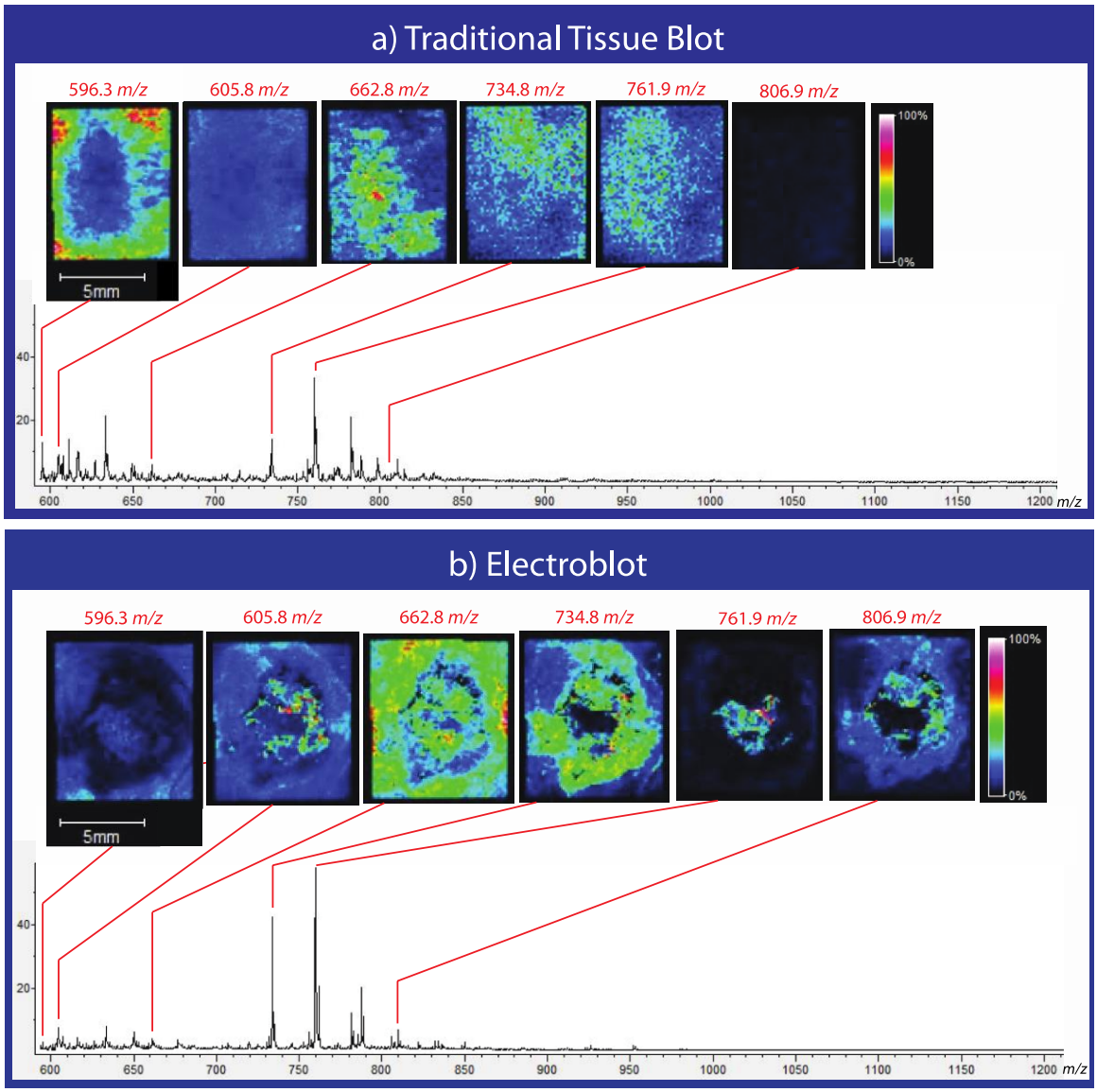

Figure 3: MALDI-TOF MSI spectra and heat maps of endogenous peptides from mouse brain tissue obtained using (a) semi-dry blotting and (b) electroblotting methods. Consecutive mouse brain tissue sections were blotted onto PVDF collection surfaces, coated with DHB, and imaged using MALDI-TOF MSI with a ±0.001% mass window. Endogenous peptides were tentatively identified from their *m/z* value by comparison with common endogenous peptides in mouse brain tissue.[30] Normalization was conducted using the total ion count for the sum of the electroblotted and semi-dry blotted samples.

Table 1: Common endogenous peptides, along with their monoisotopic *m/z* values, observed after electroblotting and semi-dry blotting of a mouse brain tissue section. Observed peptides were identified by comparison of their *m/z* values with corresponding values of common endogenous peptides identified in literature.[30] (-0.98) indicates amidation.

m/z **(Predicted; Monoisotopic)**	***m/z*** **(Observed)**	**Precursor Name**	**Sequence**
596.3164	596.3	PEBP-1	W.DGLDPGKLYTL.V
605.7728	605.8	Tachykinin-3	R.DMHDFFVGLM(-.98).G
662.8100	662.8	Corticoliberin	R.GAEDALGGHQGALE.R
734.8857	734.9	Pro-opiomelano-cortin	R.ELEGERPLGLEQV.L
761.9116	761.9	Orexin	R.LLQANGNHAAGILTM(-.98).G
806.9489	806.9	ProSAAS	L.SAASAPLVETSTPLRL.R

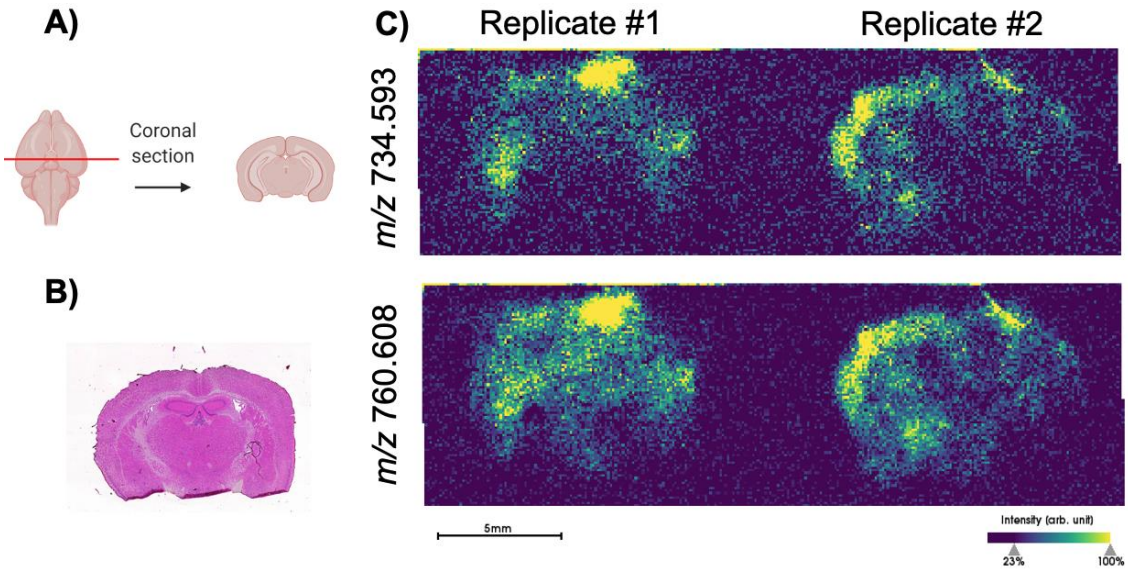

Figure 4: Two consecutive coronal mouse brain sections were examined by H&E staining and lipid distribution after electroblotting to assess lateral diffusion. A) Mouse brain schematic to illustrate the origin of the 10 µm thick sections. B) Hematoxylin and eosin (H&E) staining was performed on the first section to visualize brain structures. C) MALDI FT-ICR MSI experiments were conducted using the 15T FT-ICR at a raster size of 100 µm on the second brain section. The PVDF membrane was washed in 50 mM ammonium formate for one minute instead of the serial ethanol washes to preserve any transferred lipids after the electroblotting process. Based on accurate mass determination, diagnostic ions with the *m/z* values annotated for phosphatidylcholines PC (34:1), (*m/z* 760.609), and PC (32:0), (*m/z* 734.591), were used to illustrate the locations of the blotted tissue on the PVDF.

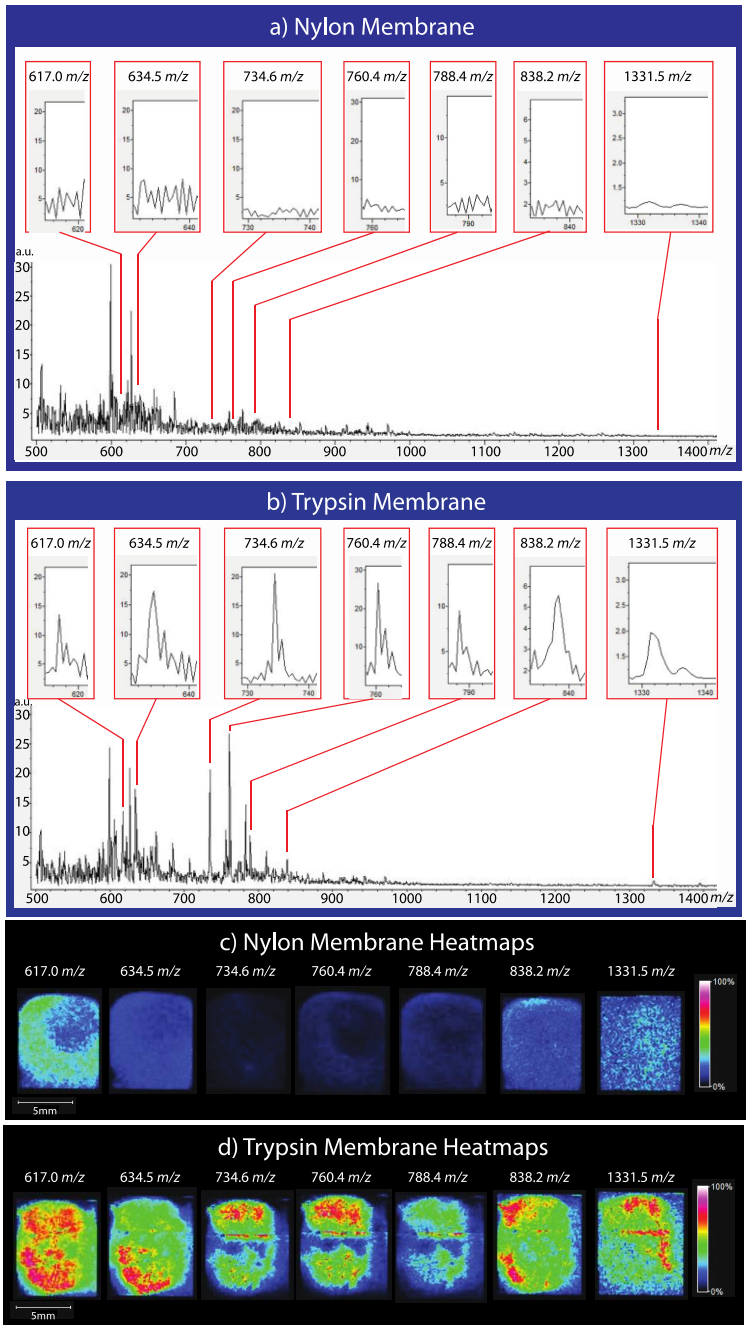

Figure 5: MALDI-TOF MSI overall average spectra of PVDF collection surfaces after electroblotting consecutive slices of mouse brain tissue through (a) bare nylon or (b) trypsin-containing nylon membranes. The analysis used a ±0.001% mass window. (c) Ion heat maps of unique peptides after electroblotting through bare nylon and (d) immobilized-trypsin membranes. Normalization was conducted using the total ion count for the sum of the electroblotted and electrodigested samples.

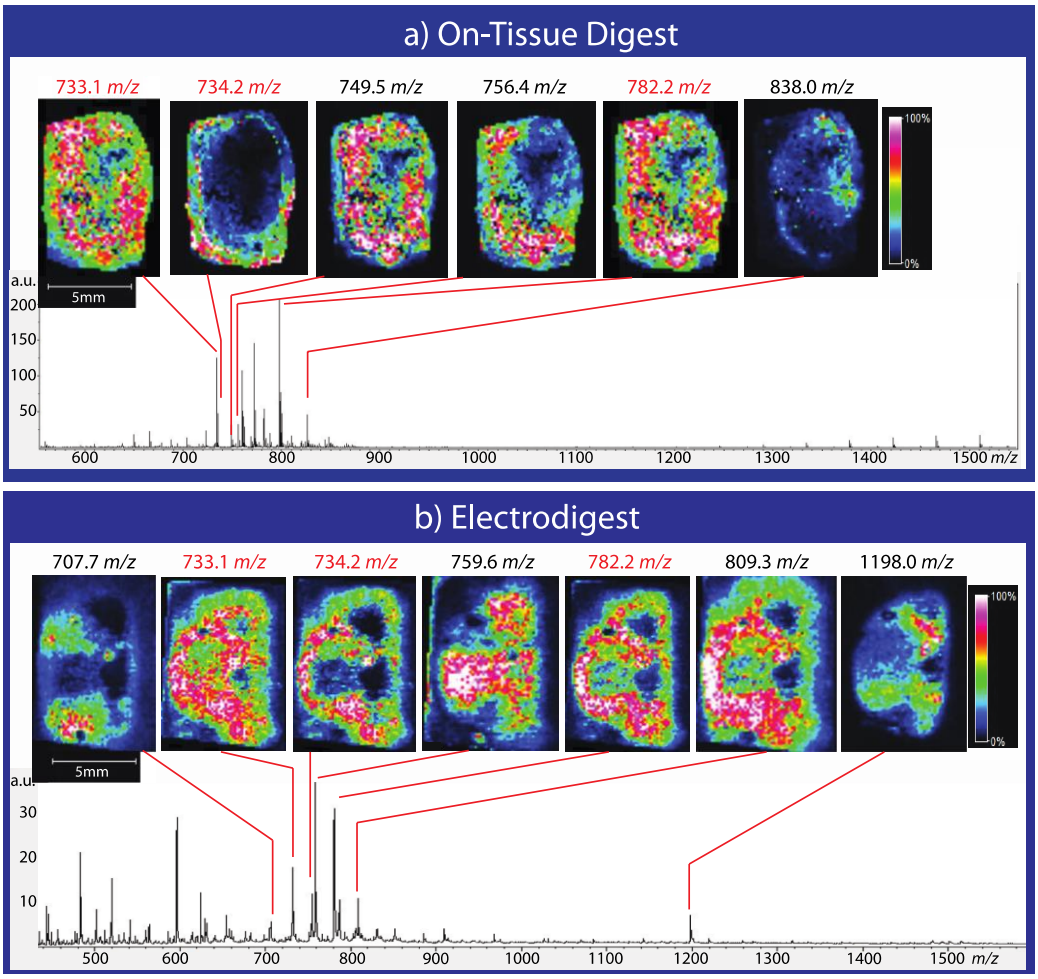

Figure 6: MALDI-TOF MSI spectra and heat maps of species from consecutive mouse brain tissue slices. Spectra and images were obtained using a) traditional on-tissue digestion and imaging and b) electrodigestion and imaging. Species of the same *m/z* that were detected in both samples are highlighted in red. Spectra were normalized using the total ion count. Different laser powers were used for the two samples, resulting in different mass ranges. The same sample was used in Figure 5b and 6b.

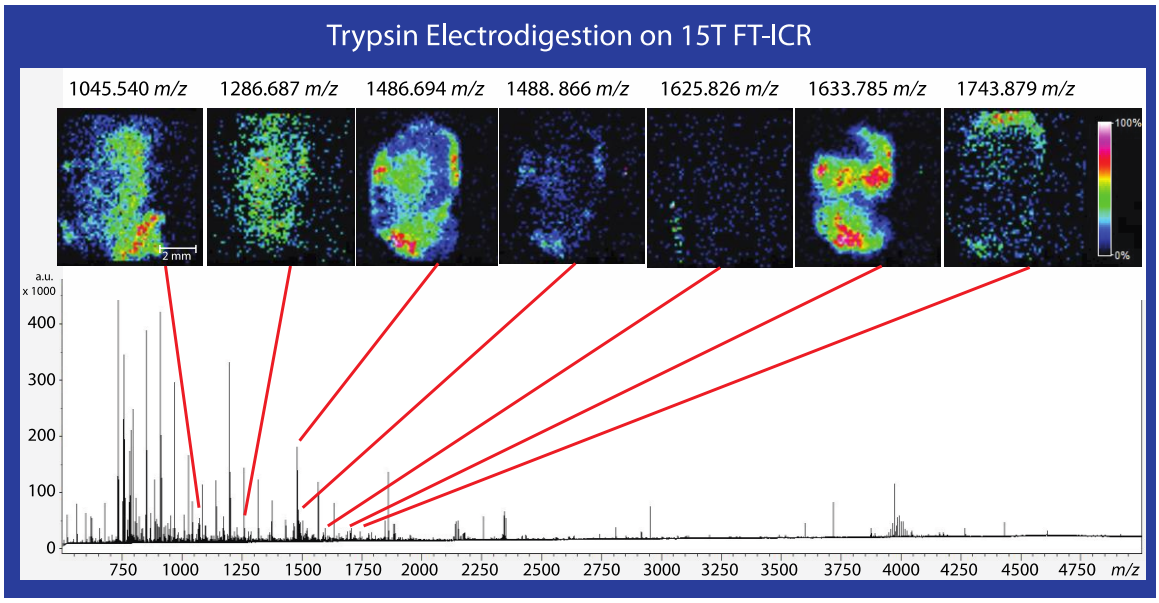

Figure 7. MALDI FT-ICR MSI overall average spectrum and heat maps corresponding to tryptic peptides from a mouse brain tissue section that was electrodigested through a trypsin membrane onto a PVDF collection surface. FT-ICR analysis yielded peaks corresponding to over 100 unique tryptic peptides. Heat maps for 1045.540, 1286.687, 1486.694, 1488.866, 1625.826, 1633 785, and 1743.879 *m/z* were chosen, as they display a wide variety of both localization and intensities for the peptides observed after MSI analysis. Ion windows of ±0.02% were used to generate ion maps. Spectra were normalized using the total ion count for all spectra in this particular sample.

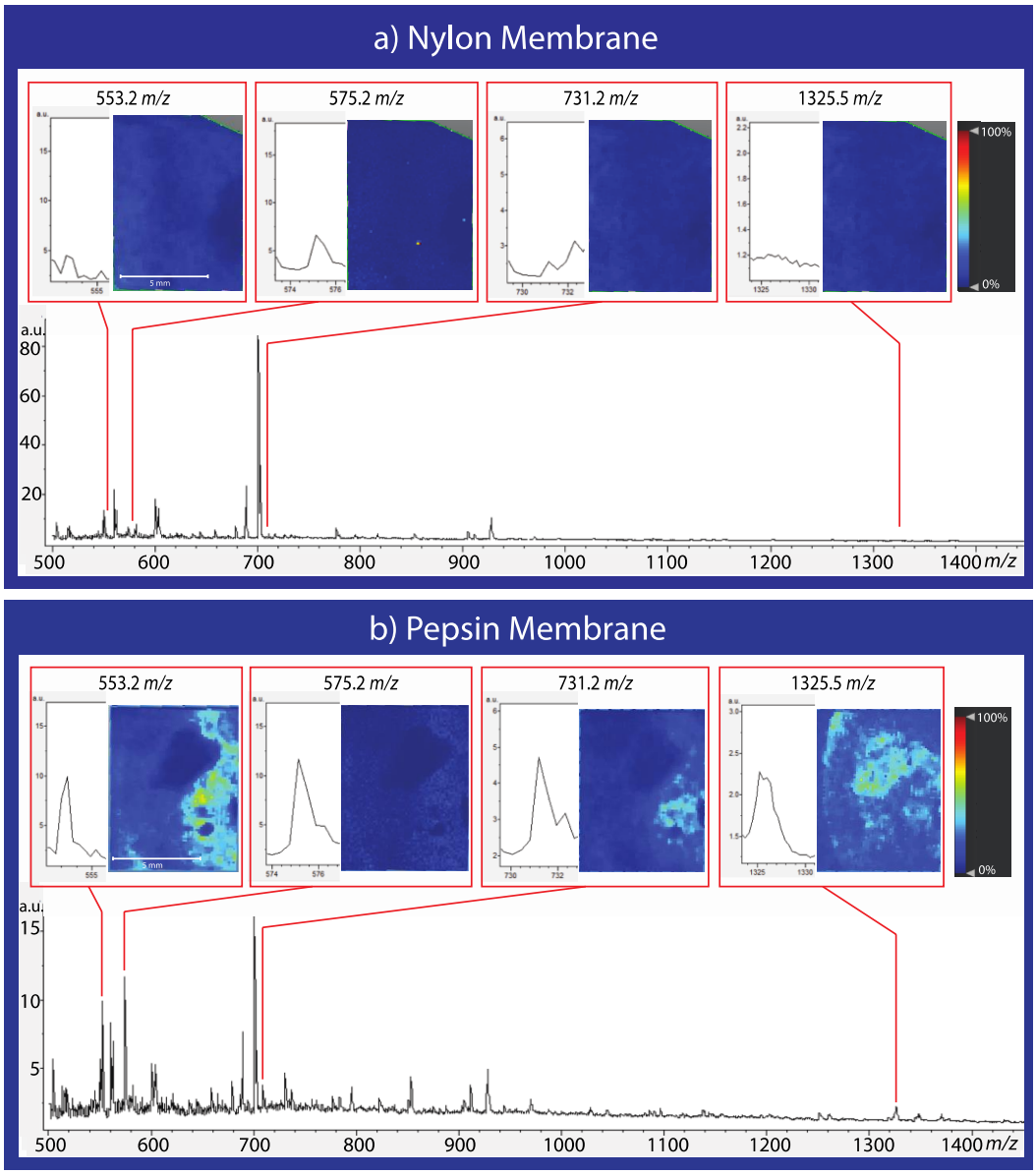

Figure 8: MALDI-TOF MSI spectra and heat maps after electroblotting a mouse brain tissue section through (a) a bare nylon membrane and (b) a membrane containing immobilized pepsin. Peaks and ion maps for four species, 553.2, 575.2, 731.2, and 1325.5 *m/z*, were compared between the two conditions. All four species appear to be present after pepsin electrodigestion and are absent after electroblotting through a bare nylon membrane. Spectra are normalized using the total ion count for each spectrum. Ion maps were generated after normalization using the total ion count for the sum of the spectra to give a more accurate comparison of relative abundance.

Associated Content:

Supporting information includes a stained brain section with lipid imaging, tentative identification of proteins and peptides, as well as peptides corresponding to the autolysis of trypsin and associated MS/MS spectra. Additional supplemental information includes a spectral comparison of a PVDF collection surface after electroblotting a mouse brain tissue section through a bare nylon membrane versus a membrane containing immobilized pepsin and a spectral comparison of BSA before and after electroblotting to illustrate the effect of the process on spatial diffusion of peptides.

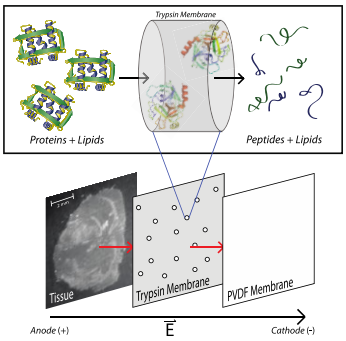

Table of Contents Figure

References:

1. Mezger, S. T. P.; Mingels, A. M. A.; Bekers, O.; Heeren, R. M. A.; Cillero-Pastor, B., Mass Spectrometry Spatial-Omics on a Single Conductive Slide. *Anal Chem* **2021**.
2. Berghmans, E.; Boonen, K.; Maes, E.; Mertens, I.; Pauwels, P.; Baggerman, G., Implementation of MALDI Mass Spectrometry Imaging in Cancer Proteomics Research: Applications and Challenges. *J Pers Med* **2020,** *10* (2).
3. Vu, N. Q.; DeLaney, K.; Li, L., Neuropeptidomics: Improvements in Mass Spectrometry Imaging Analysis and Recent Advancements. *Curr Protein Pept Sci* **2020**.
4. Hummon, A. B.; Amare, A.; Sweedler, J. V., Discovering new invertebrate neuropeptides using mass spectrometry. *Mass Spectrom Rev* **2006,** *25* (1), 77-98.
5. LaBonia, G. J.; Lockwood, S. Y.; Heller, A. A.; Spence, D. M.; Hummon, A. B., Drug penetration and metabolism in 3D cell cultures treated in a 3D printed fluidic device: assessment of irinotecan via MALDI imaging mass spectrometry. *Proteomics* **2016,** *16* (11-12), 1814-21.
6. Liu, X.; Hummon, A. B., Chemical Imaging of Platinum-Based Drugs and their Metabolites. *Sci Rep* **2016,** *6*, 38507.
7. Liu, X.; Weaver, E. M.; Hummon, A. B., Evaluation of therapeutics in three-dimensional cell culture systems by MALDI imaging mass spectrometry. *Anal Chem* **2013,** *85* (13), 6295-302.
8. Ryan, D. J.; Spraggins, J. M.; Caprioli, R. M., Protein identification strategies in MALDI imaging mass spectrometry: a brief review. *Curr Opin Chem Biol* **2019,** *48*, 64-72.
9. Zink, K. E.; Dean, M.; Burdette, J. E.; Sanchez, L. M., Imaging Mass Spectrometry Reveals Crosstalk between the Fallopian Tube and the Ovary that Drives Primary Metastasis of Ovarian Cancer. *ACS Cent Sci* **2018,** *4* (10), 1360-1370.
10. Zubair, F.; Laibinis, P. E.; Swisher, W. G.; Yang, J.; Spraggins, J. M.; Norris, J. L.; Caprioli, R. M., Trypsin and MALDI matrix pre-coated targets simplify sample preparation for mapping proteomic distributions within biological tissues by imaging mass spectrometry. *J Mass Spectrom* **2016,** *51* (12), 1168-1179.
11. Rohner, T. C.; Staab, D.; Stoeckli, M., MALDI mass spectrometric imaging of biological tissue sections. *Mech Ageing Dev* **2005,** *126* (1), 177-85.
12. Wang, M. Z.; Fitzgerald, M. C., A solid sample preparation method that reduces signal suppression effects in the MALDI analysis of peptides. *Anal Chem* **2001,** *73* (3), 625-31.
13. Annesley, T. M., Ion suppression in mass spectrometry. *Clin Chem* **2003,** *49* (7), 1041-4.
14. Diehl, H. C.; Beine, B.; Elm, J.; Trede, D.; Ahrens, M.; Eisenacher, M.; Marcus, K.; Meyer, H. E.; Henkel, C., The challenge of on-tissue digestion for MALDI MSI- a comparison of different protocols to improve imaging experiments. *Anal Bioanal Chem* **2015,** *407* (8), 2223-43.
15. Albrethsen, J., Reproducibility in protein profiling by MALDI-TOF mass spectrometry. *Clin Chem* **2007,** *53* (5), 852-8.
16. Bickner, A. N.; Champion, M. M.; Hummon, A. B.; Bruening, M. L., Electroblotting through a tryptic membrane for LC-MS/MS analysis of proteins separated in electrophoretic gels. *Analyst* **2020,** *145* (23), 7724-7735.
17. Binz, P. A.; Muller, M.; Hoogland, C.; Zimmermann, C.; Pasquarello, C.; Corthals, G.; Sanchez, J. C.; Hochstrasser, D. F.; Appel, R. D., The molecular scanner: concept and developments. *Curr Opin Biotechnol* **2004,** *15* (1), 17-23.

18. Luxembourg, S. L.; Vaezaddeh, A. R.; Amstalden, E. R.; Zimmermann-Ivol, C. G.; Hochstrasser, D. F.; Heeren, R. M., The molecular scanner in microscope mode. *Rapid Commun Mass Spectrom* **2006,** *20* (22), 3435-42.
19. Bienvenut, W. V.; Sanchez, J. C.; Karmime, A.; Rouge, V.; Rose, K.; Binz, P. A.; Hochstrasser, D. F., Toward a clinical molecular scanner for proteome research: parallel protein chemical processing before and during western blot. *Anal Chem* **1999,** *71* (21), 4800-7.
20. Dong, J.; Ning, W.; Liu, W.; Bruening, M. L., Limited proteolysis in porous membrane reactors containing immobilized trypsin. *Analyst* **2017,** *142* (14), 2578-2586.
21. Xu, F.; Wang, W.-H.; Tan, Y.-J.; Bruening, M. L., Facile Trypsin Immobilization in Polymeric Membranes for Rapid, Efficient Protein Digestion. *Analytical Chemistry* **2010,** *82* (24), 10045-10051.
22. Tan, Y.-J.; Wang, W.-H.; Zheng, Y.; Dong, J.; Stefano, G.; Brandizzi, F.; Garavito, R. M.; Reid, G. E.; Bruening, M. L., Limited Proteolysis via Millisecond Digestions in Protease-Modified Membranes. *Analytical Chemistry* **2012,** *84* (19), 8357-8363.
23. Andrews, W. T.; Skube, S. B.; Hummon, A. B., Magnetic bead-based peptide extraction methodology for tissue imaging. *Analyst* **2017,** *143* (1), 133-140.
24. Weston, L. A.; Bauer, K. M.; Skube, S. B.; Hummon, A. B., Selective, bead-based global peptide capture using a bifunctional cross-linker. *Anal Chem* **2013,** *85* (22), 10675-9.
25. Fournaise, E.; Chaurand, P., Increasing specificity in imaging mass spectrometry: high spatial fidelity transfer of proteins from tissue sections to functionalized surfaces. *Anal Bioanal Chem* **2015,** *407* (8), 2159-66.
26. Groseclose, M. R.; Andersson, M.; Hardesty, W. M.; Caprioli, R. M., Identification of proteins directly from tissue: in situ tryptic digestions coupled with imaging mass spectrometry. *J Mass Spectrom* **2007,** *42* (2), 254-62.
27. Pang, Y.; Wang, W.-H.; Reid, G. E.; Hunt, D. F.; Bruening, M. L., Pepsin-Containing Membranes for Controlled Monoclonal Antibody Digestion Prior to Mass Spectrometry Analysis. *Analytical Chemistry* **2015,** *87* (21), 10942-10949.
28. Bhattacharjee, S.; Dong, J.; Ma, Y.; Hovde, S.; Geiger, J. H.; Baker, G. L.; Bruening, M. L., Formation of high-capacity protein-adsorbing membranes through simple adsorption of poly(acrylic acid)-containing films at low pH. *Langmuir* **2012,** *28* (17), 6885-92.
29. Schneider, C. A.; Rasband, W. S.; Eliceiri, K. W., NIH Image to ImageJ: 25 years of image analysis. *Nat Methods* **2012,** *9* (7), 671-5.
30. Zhang, X.; Petruzziello, F.; Zani, F.; Fouillen, L.; Andren, P. E.; Solinas, G.; Rainer, G., High identification rates of endogenous neuropeptides from mouse brain. *J Proteome Res* **2012,** *11* (5), 2819-27.
31. Kaya, I.; Samfors, S.; Levin, M.; Boren, J.; Fletcher, J. S., Multimodal MALDI Imaging Mass Spectrometry Reveals Spatially Correlated Lipid and Protein Changes in Mouse Heart with Acute Myocardial Infarction. *J Am Soc Mass Spectrom* **2020,** *31* (10), 2133-2142.
32. Heijs, B.; Carreira, R. J.; Tolner, E. A.; de Ru, A. H.; van den Maagdenberg, A. M.; van Veelen, P. A.; McDonnell, L. A., Comprehensive analysis of the mouse brain proteome sampled in mass spectrometry imaging. *Anal Chem* **2015,** *87* (3), 1867-75.